3 Results

3.1 Patient K030 Displayed Potent Anti-Tumour Immune Responses Following Vaccination

Patient K030, a female caucasian born on 31/05/1942, was initially diagnosed with adenocarcinoma of the breast in 1990. After treatment with high dose chemotherapy and peripheral blood stem cell support for pulmonary metastases, K030 showed a complete response. In May 1996 it was discovered that the patient had melanoma metastases in subcutaneous tissues, lymph nodes and intestine. Subsequently K030 was enrolled in a retroviral vaccine trial with autologous irradiated melanoma cells genetically engineered to secrete GM-CSF [161]. Several soft tissue lesions were surgically removed. The tissue was processed into single cell suspension and a short-term tissue culture was established. The patient's melanoma cells were transduced with pMFG-GM-CSF retroviral particle supernatants derived from CRIP packaging cells. The transduced melanoma cells were cryopreserved.

The patient was given 12 half-intradermal, half-subcutaneous injections on a weekly basis from October 1996 to January 1997. A partial regression of subcutaneous metastases was observed. In Febuary 1997 a colonic metastasis had to be surgically removed. Pathologic examination of the resected tissue showed that the metastasis was largely necrotic and heavily infiltrated by lymphocytes. Antibody staining showed large numbers of $CD4^+$ and $CD8^+$ T lymphocytes as well as $CD20^+$ B cells (Fig. 1 A-C. The tissue sections were processed in the laboratory of our collaborating pathologist Martin C. Mihm Jr.). Necrosis and brisk lymphocytic infiltrates were seen in resected metastases in 11 out of 16 biopsied patients.

K030 received 12 additional doses of the vaccine until November 1997. In September 1998 a new cystic calf metastasis caused the patient pain. The tumour was resected. Again, pathologic analysis showed extensive necrosis of the tumour and dense lymphocytic infiltrates (Fig. 1 D-F).

Since the retroviral trial had been closed at this time the patient was enrolled in an adenoviral trial [162]. The resected tissue was processed into single cell suspension and transduced with a replication defective adenoviral vector encoding human GM-CSF. Up to February 1999 the patient received 11 doses when the calf metastasis recurred and subsequently became indurated. It was not possible to obtain a tissue specimen but the metastasis was clinically evaluated as progressive cancer.

The patient received treatment in the form of isolated limb perfusion TNF-α, melphalan, surgical removal of a residual necrotic mass and radiation therapy. Furthermore, two subcutaneous lesions were removed in November and December 1999. Both lesions were largely necrotic and heavily infiltrated by lymphocytes.

The resected tissue was infected with adenoviral particles to produce a third batch of vaccine. The patient received an additional 18 doses of this vaccine between March and September 2000. At this point a metastasis obstructed the small bowel and had to be surgically removed. Upon pathological examination of the resected tumour tissue it was noted that neither necrotic tissue nor lymphocyte infiltrates were present. Tumour cells derived from this metastases were adenovirally transduced for a fourth vaccine preparation. The patient received a final round of four vaccinations, but subsequently disease progressed and the patient died in March 2001.

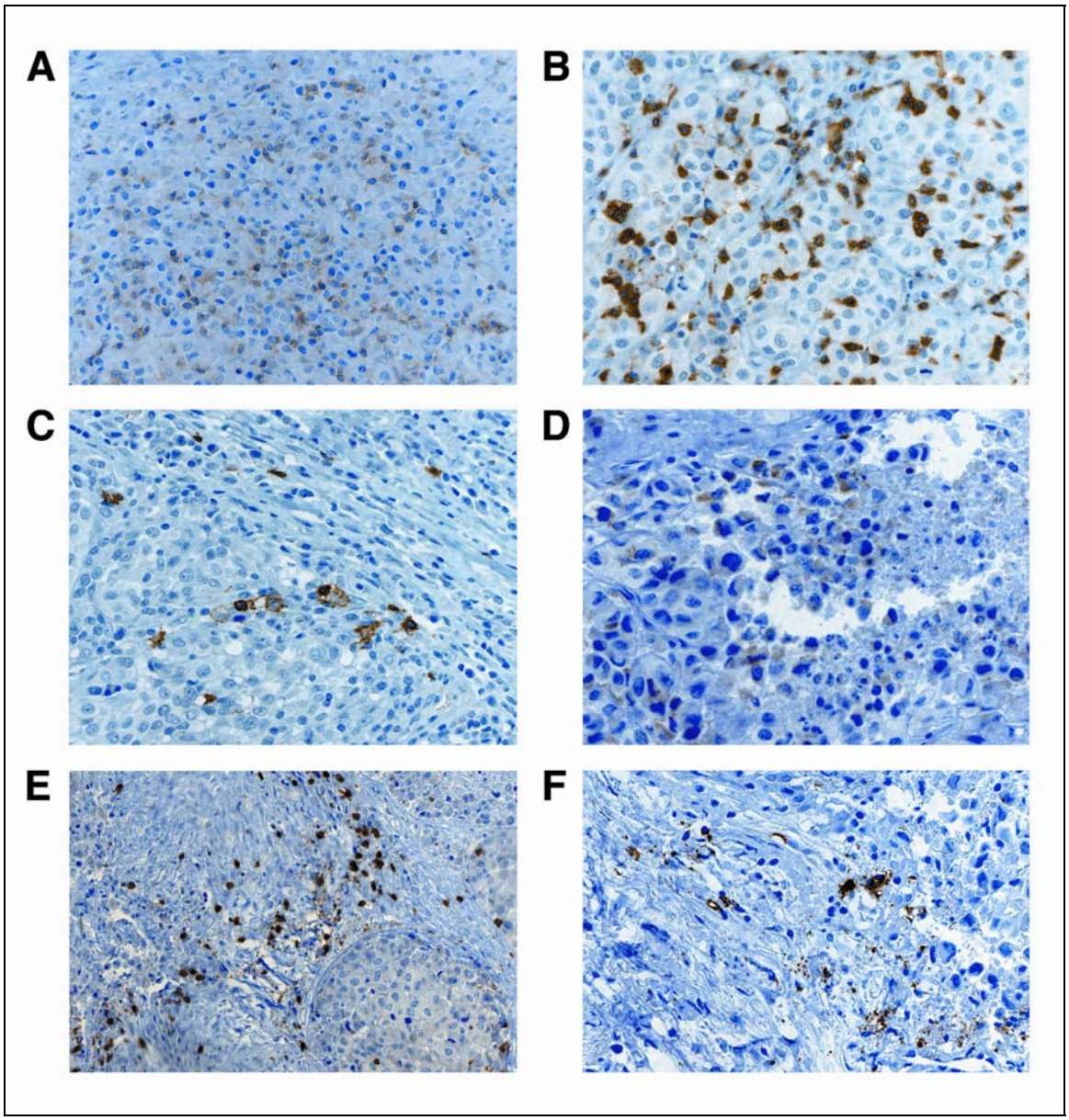

Figure 1. Infiltrated metastases from late stage melanoma patient K030 with extensive tumour destruction following vaccination with autologous, irradiated GM-CSF secreting melanoma cells. Paraffin-embedded tissue sections were probed with different antibodies and counterstained with hematoxylin. A-C, colon metastasis; D-F, calf metastasis. (**A**) $CD4^+$ T cells. (**B**) $CD8^+$ T cells. (**C**) $CD20^+$ B cells. (**D**) $CD4^+$ T cells. **(E)** $CD8^+$ T cells. **(F)** $CD20^+$ B cells.

3.2 Identification of the Novel IAP Family Member ML-IAP as a Target for the Immune Response

We wanted to identify the antigenic targets of the immune response in patient K030 that elicited widespread tumour necrosis. In previous studies we had shown that post-vaccination serum displayed an increase of antibody reactivity against melanoma determinants as seen in immunoblotting and flow cytometry [161]. We therefore decided to screen a melanoma expression library with serum obtained after treatment began in order to discover potential tumour regression antigens.

The resected soft tissue lesions from K030 that had been used in short term tissue culture for generating the first batch of the vaccine did not yield a stable cell line. Thus, we were unable to construct a cDNA expression library from K030's melanoma cells. Instead we screened a phage expression library constructed with melanoma-derived cDNA from another patient on the trial. (This library had been made by F. Stephen Hodi Jr. in our group.) This patient, K008, also displayed widespread tumour necrosis and brisk lymphocte infiltrates in distant metastases. Despite being diagnosed with recurring melanoma in 1993 after a primary lesion had been removed from the patient's arm in 1991, K008 remains virtually disease-free in the autumn of 2003.

When we screened the expression library with serum derived three months after the first round of vaccination we identified several cDNA inserts that coded for proteins which were recognised by IgG antibodies in the patient's plasma (Table 1). An especially strong signal was seen with phage clone 14.1 (Fig. 2) which contained a 1246 base pair (bp) insert with an at the time unknown sequence (Fig. 3).

Closer analysis of the predominant open reading frame (ORF) in this insert showed that a stop codon was preceeding two potential initiator methionines. The first methionine was located 57 bp downstream of the stop codon within a nucleotide sequence that bore significant correlation with the Kozak consensus sequence [167] and was determined to be the likely start of the 840 bp long ORF.

Therefore we concluded that we had identified the full sequence of a protein with 280 amino acids.

To identify the insert's sequence we performed homology searches in the National Center for Biotechnology Information (NCBI) database with the Basic Local Alignment Search Tool (BLAST)[168]. A search with the full nucleotide sequence did not yield significant matches. An expressed sequence tag (EST) search showed almost perfect alignment with a short cDNA derived from melanoma, affirming that the discovered protein was expressed in this type of malignancy. BLAST analysis with the potential amino acid sequences, however, showed high homology with members of the recently discovered family of inhibitor of apoptosis proteins (IAPs)(reviewed in [169-171]), most notably with human X-linked inhibitor of apoptosis protein (XIAP)[172](Fig. 4).

Name of Protein	**Function of Protein**
Melanoma inhibitor of apoptosis protein (ML-IAP)	ML-IAP interacts with caspases and protects cells from a wide variety of apoptotic stimuli [173, 174].
Mind bomb (Mib)	Mib is an ubiquitin ligase essential for activation of notch signalling by delta [175].
Universal binding factor 2 (UBF2)	UBF2 is a RNA polymerase II transcription factor. One of its functions is to enhance the β-catenin signalling pathway [176]. This pathway can drive the malignant transformation of cells.
Tyrosinase related protein 2 (Trp2)	Trp2 belongs to the group of melanocyte differentiation antigens, proteins involved in the production of melanin. Trp2 is a known TAA [37, 60].

Table 1. Overview of the proteins recognised by patient K030's IgG antibodies after screening a melanoma-based cDNA expression library with post-vaccination serum. The identified differentiation antigen Trp2 is a well-known TAA. ML-IAP's role as a tumour-associated antigen is described in this thesis, the detailed analysis of the other identified proteins is still ongoing.

The phage insert's putative ORF clearly had a single N-terminal baculovirus IAP repeat (BIR) domain that defines membership in this particular family of caspase antagonists and an C-terminal "really interesting new gene" (RING) domain that is present in several other IAPs. Both domains are zinc coordinating motifs and have highly evolutionary conserved cysteine and histidine residues.

IAPs were first discovered by a genetic complementation assay for apoptosis inhibitor p35 in baculoviruses [177-179]. It became soon apparent that IAPs are highly evolutionary conserved and expressed in organisms ranging from yeast [180] and nematodes [181] to mammals [182]. In contrast to other viral apoptosis inhibitors like p35 [183] and cowpox virus-derived cytokine response modifier A (CrmA) [184] which both mimic caspase substrates, IAPs interact with caspases through their BIR domains and BIR linker regions [185, 186] and counteract a wider variety of apoptotic stimuli. The BIR domain is present in one to three copies and contains the DX_3CXC and HX_6C consensus motifs.

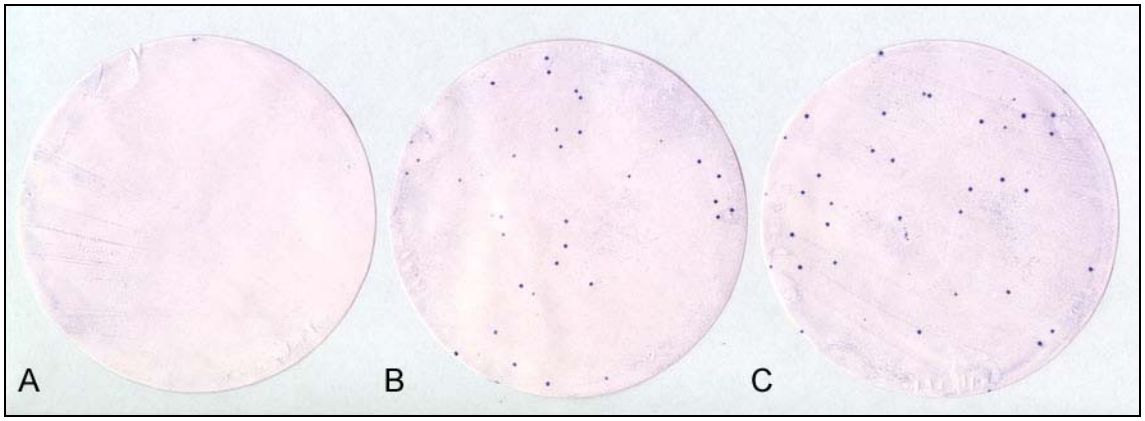

Figure 2. Specific detection of the protein expressed by phage clone 14.1 infected *E. coli* with serum from patient K030. Plaques were blotted on nitrocellulose membranes and incubated with serum derived 3 months post-vaccination at 1:1,000 in TTBS. A Fcγ-specific alkaline phosphatase-labelled secondary polyclonal antibody was used to detect antigen specific IgG. **(A)** Membrane with several hundred plaques derived from an empty control library. **(B)** Membrane with a mix of several hundred plaques from the empty control library and a low number of plaques from purified phage clone 14.1. **(C)** Membrane with plaques from purified phage clone 14.1 only.

RING domains are present in several human IAPs and several hundred other proteins. This domain functions as an E3 ubiquitin-protein isopeptide ligase (ubiquitin ligases) in the ubiquitination pathway, i. e. it transfers ubiquitin to a protein target which subsequently leads to proteosomal degradation [187]. There is experimental evidence that RING domains regulate expression levels of IAPs by autoubiquitination and caspases and IAP antagonists by ubiquitination [188-191].

In order to determine the tissue expression pattern of this new IAP family member we probed a commercially available multi tissue Northern blot (Clontech) with full length 840 bp cDNA (Fig. 5). The blot revealed a highly restricted expression pattern with only testis, spinal cord, lymph node and placenta displaying a signal. While the testis lane yielded a diffuse signal between 2.3 and 4.4 kb, spinal cord, lymph node and placenta displayed 3 transcripts at circa 1.5 kb, 2.3 kb and 3.5 kb. Spinal cord-derived mRNA showed an additional transcript below 1.25 kb.

Next, it was necessary to ensure that we had identified the normal sequence of the novel IAP since proteins expressed in cancer cells have a higher probability of carrying mutations. Because our melanoma-derived sequence could not be independently verified with a database entry, we had to obtain sequence information from normal tissue. After analysing the expression pattern in normal tissue we obtained with the Northern blot (Fig. 5), we decided to carry out a hybridisation screening with a commercially available placenta-derived phage expression library (Stratagene). ^{32}P-labelled ML-IAP DNA was hybrised to $1x10^6$ denatured bacterial plaques on nylon membranes in duplicate. After several rounds of screening a phagemid with full length cDNA was isolated. The coding region found was identical to the one in the melanoma expression library, thereby confirming the sequence of the novel IAP.

```
5′UTR
CGGCACGAGCTCGTGCCGGGCAGGCCTGTGCCTATCCCTGCTGTCCCCAGGGTGGGCCCCGGGGGTCAGGAGCTCCAGA
AGGGCCAGCTGGGCATATTCTGAGATTGGCCATCAGCCCCCATTTCTGCTGCAAACCTGGTCAGAGCCAGTGTTCCCTC
C
1/1                                             31/11
ATG GGA CCT AAA GAC AGT GCC AAG TGC CTG CAC CGT GGA CCA CAG CCG AGC CAC TGG GCA
M   G   P   K   D   S   A   K   C   L   H   R   G   P   Q   P   S   H   W   A
61/21                                           91/31
GCC GGT GAT GGT CCC ACG CAG GAG CGC TGT GGA CCC CGC TCT CTG GGC AGC CCT GTC CTA
A   G   D   G   P   T   Q   E   R   C   G   P   R   S   L   G   S   P   V   L
121/41                                          151/51
GGC CTG GAC ACC TGC AGA GCC TGG GAC CAC GTG GAT GGG CAG ATC CTG GGC CAG CTG CGG
G   L   D   T   C   R   A   W   D   H   V   D   G   Q   I   L   G   Q   L   R
181/61                                          211/71
CCC CTG ACA GAG GAG GAA GAG GAG GAG GGC GCC GGG GCC ACC TTG TCC AGG GGG CCT GCC
P   L   T   E   E   E   E   E   E   G   A   G   A   T   L   S   R   G   P   A
241/81                                          271/91
TTC CCC GGC ATG GGC TCT GAG GAG TTG CGT CTG GCC TCC TTC TAT GAC TGG CCG CTG ACT
F   P   G   M   G   S   E   E   L   R   L   A   S   F   Y   D   W   P   L   T
301/101                                         331/111
GCT GAG GTG CCA CCC GAG CTG CTG GCT GCT GCC GGC TTC TTC CAC ACA GGC CAT CAG GAC
A   E   V   P   P   E   L   L   A   A   A   G   F   F   H   T   G   H   Q   D
361/121                                         391/131
AAG GTG AGG TGC TTC TTC TGC TAT GGG GGC CTG CAG AGC TGG AAG CGC GGG GAC GAC CCC
K   V   R   C   F   F   C   Y   G   G   L   Q   S   W   K   R   G   D   D   P
421/141                                         451/151
TGG ACG GAG CAT GCC AAG TGG TTC CCC AGC TGT CAG TTC CTG CTC CGG TCA AAA GGA AGA
W   T   E   H   A   K   W   F   P   S   C   Q   F   L   L   R   S   K   G   R
481/161                                         511/171
GAC TTT GTC CAC AGT GTG CAG GAG ACT CAC TCC CAG CTG CTG GGC TCC TGG GAC CCG TGG
D   F   V   H   S   V   Q   E   T   H   S   Q   L   L   G   S   W   D   P   W
541/181                                         571/191
GAA GAA CCG GAA GAC GCA GCC CCT GTG GCC CCC TCC GTC CCT GCC TCT GGG TAC CCT GAG
E   E   P   E   D   A   A   P   V   A   P   S   V   P   A   S   G   Y   P   E
601/201                                         631/211
CTG CCC ACA CCC AGG AGA GAG GTC CAG TCT GAA AGT GCC CAG GAG CCA GGA GCC AGG GAT
L   P   T   P   R   R   E   V   Q   S   E   S   A   Q   E   P   G   A   R   D
661/221                                         691/231
GTG GAG GCG CAG CTG CGG CGG CTG CAG GAG GAG AGG ACG TGC AAG GTG TGC CTG GAC CGC
V   E   A   Q   L   R   R   L   Q   E   E   R   T   C   K   V   C   L   D   R
721/241                                         751/251
GCC GTG TCC ATC GTC TTT GTG CCG TGC GGC CAC CTG GTC TGT GCT GAG TGT GCC CCC GGC
A   V   S   I   V   F   V   P   C   G   H   L   V   C   A   E   C   A   P   G
781/261                                         811/271
CTG CAG CTG TGC CCC ATC TGC AGA GCC CCC GTC CGC AGC CGC GTG CGC ACC TTC CTG TCC
L   Q   L   C   P   I   C   R   A   P   V   R   S   R   V   R   T   F   L   S
841/281
TAG
*
3′UTR
GCCAGGTGCCATGGCCGGCCAGGTGGGCTGCAGAGTGGGCTCCCTGCCCCTCTCTGCCTGTTCTGGACTGTGTTCTGGG
CCTGCTGAGGATGGCAGAGCTGGTGTCCATCCAGCACTGACCAGCCCTGATTCCCCGACCACCGCCCAGGGTGGAGAAG
GAGGCCCTTGCTTGGCGTGGGGGATGGCTTAACTGTACCTGTTTGGATGCTTCTGAATAGAAATAAAGTGGGTTTTCCC
TGGAGGT
```

Figure 3. cDNA insert from phage clone 14.1 which contains the full length 840 bp ORF sequence along with 5' and 3' untranslated regions (UTRs) for the 280 amino acid variant of the novel inhibitor of apoptosis protein now known as ML-IAP. The baculoviral IAP repreat (BIR) domain is marked by red letters, the "really interesting new gene" (RING) domain is marked by blue letters.

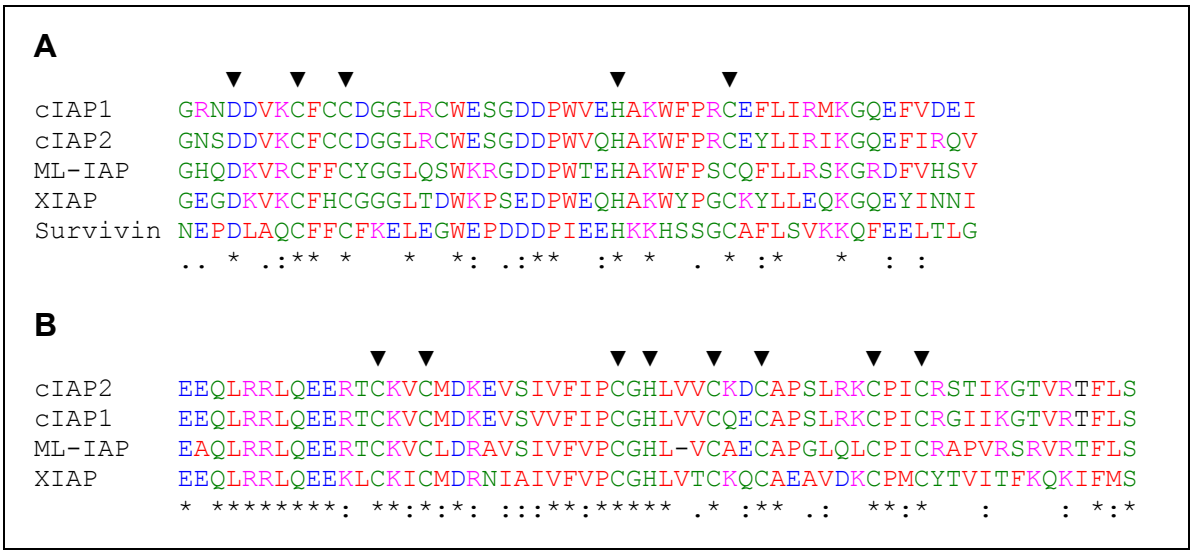

Figure 4. Sequence comparison showed that the novel protein ML-IAP recognised by the humoral response of patient K030 is a member of the IAP protein family. Pile-up performed with the Clustal W programme [192]. The residues of the consensus motif are marked with an "▼". **(A)** Conserved part of the baculoviral IAP repeat (BIR) domain. The BIR domains along with their linker regions interact with caspases and are necessary for inhibition of apoptosis. **(B)** Really interesting new gene (RING) domain. RING domains are involved in ubiquitination.

"*" denotes an identical residue, ":" denotes a conserved substitution and "." denotes a semi-conserved substitution. The colour red denotes small (small + hydrophobic (incl. aromatic - Y)) amino acids, blue denotes acidic amino acids, magneta denotes basic amino acids and green denotes hydroxyl + amine + basic – Q amino acids.

During our investigation this new IAP family member was independently discovered by three other groups that carried out database homology searches and is now called ML-IAP (for melanoma IAP)[173] but was also described as livin [174] and KIAP (This group obtained the full sequence from a kidney-based library.)[193]. The functional studies carried out in these laboratories confirmed that expression of ML-IAP renders cells less vulnerable to a wide variety of apoptotic stimuli such as cytotoxic reagents (e. g. adriamycin, 4-tertiary butylphenol) and expression of death receptors (e. g. DR4, DR5, DR6, Fas and TNFR1). *In vitro* studies showed that ML-IAP inhibits caspases 9 and 3. It is currently controversial whether IAP also binds caspase 7 [173, 174]. ML-IAP is also known to activate JNK1 [194].Furthermore, ML-IAP can be blocked by the

IAP antagonists Smac/Diablo [195] and Omi/HtrA2 [196]. Both of these factors are released by mitochondria and interact with IAPs through their IAP binding motifs (IBMs) which consist of a four amino acid sequence lead by alanine. Omi/HtrA2 has been shown to cleave several IAPs, including ML-IAP [196]. These results have been substantiated by similar findings in the model organism *Drosophila melanogaster* where the genes head-involution defective (hid) [197], grim [198], Reaper (rpr) [191, 198, 199], sickle (skl) [200] and jafrac2 [201] encode functional homologues of Smac/DIABLO and Omi/HtrA2. These proteins bind to *Drosophila* IAP1 (DIAP1) via the rpr-hid-grim (RHG) motif and prevent it from inhibiting the *Drosophila* caspase DRONC [202, 203].

A second, 298 residue long ML-IAP variant was described by Vucic *et al.* [173]. While this laboratory found no difference between the two splice variants in their antiapoptotic function, Ashab *et al.* provided data that showed significant disparity when cells transfected with the two ML-IAP forms were exposed to staurosporine and etoposide [204]. Functional studies have been predominantly focussed on the 280 aa form so far.

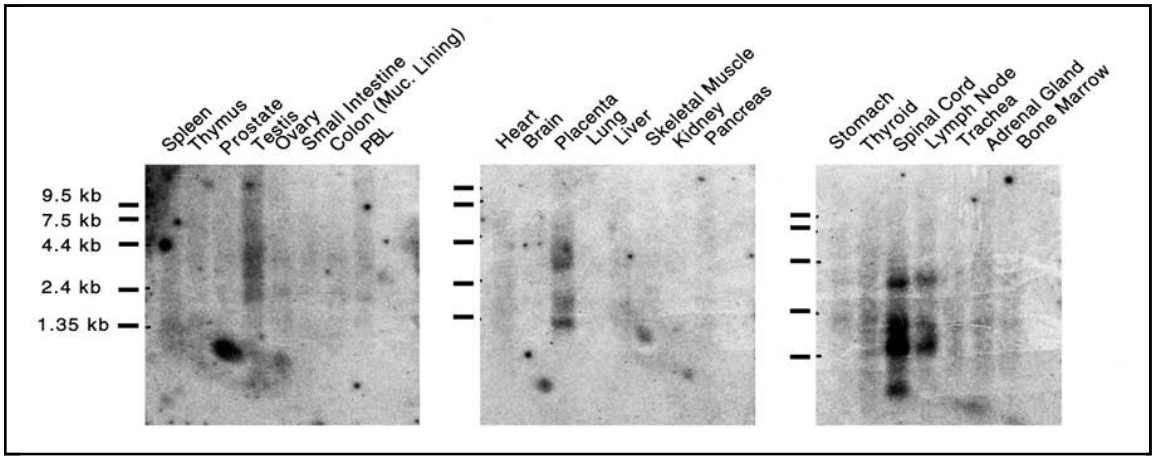

Figure 5. Multi tissue Northern blot probed with ^{32}P-labelled ML-IAP cDNA (840 bp, full ORF of 280 aa variant). ML-IAP expression is highly restricted in normal tissue. Transcripts of several sizes can be seen in spinal cord, lymph node, placenta and testis. The cDNA insert identified by serological screening was 1246 in length, including 5' and 3' UTR.

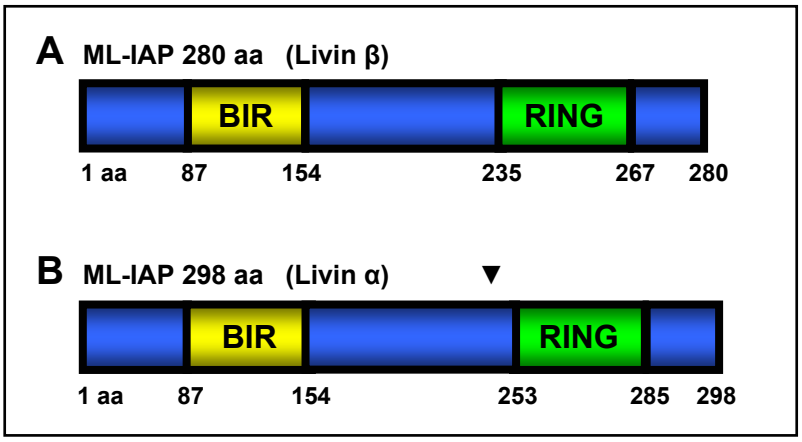

Figure 6. Schematic view of the two currently known splice variants of ML-IAP. **(A)** The 280 aa form of ML-IAP (occasionally referred to as Livin β) has a single BIR and a single RING domain connected by a 81 aa linker region. **(B)** The 298 aa form (Livin α) has an additional 18 residues right before the RING domain (arrowhead).

3.3 Vaccination Increases ML-IAP-Specific Antibody Titres and Induces Isotype Switching

After establishing that the patient had significant levels of antibodies recognising ML-IAP, we were interested in studying the changes in antibody concentration over the course of treatment. In order to link changes in the ML-IAP-specific humoral response to vaccine administration and clinical history we established an ELISA.

All available plasma samples from patient K030's 33 timepoints, including one sample that was taken prior to the administration of the vaccine, contained high titre IgG antibody against recombinant GST-ML-IAP (Fig. 8A) but no IgG antibody against GST alone (data not shown). Several bloody aspirates from the patient's necrotic and infiltrated calf metastasis that had been taken at different timepoints showed similar antibody levels (data not shown). The signal for overall anti-ML-IAP IgG was still detectable at a dilution of 1:50,000.

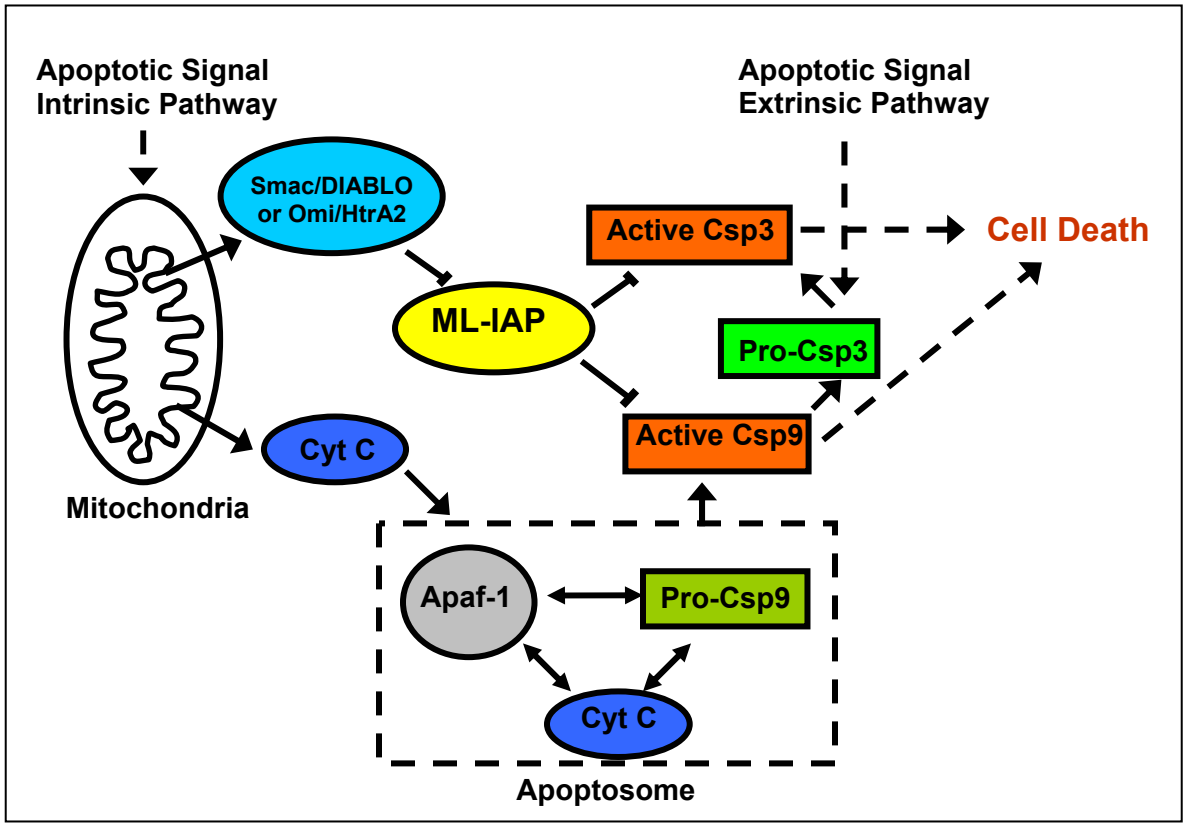

Figure 7. Current model for the function of ML-IAP. ML-IAP has been shown to block signalling through the intrinsic and extrinsic apoptotic pathways by inhibiting apical caspase 9 and executioner caspase 3. Smac/DIABLO and Omi/HtrA2 are ML-IAP antagonists that are released by mitochondria. They interact with IAP family members through the IAP binding motif (IBM), a four aa sequence. The capacity to block downstream executioner caspase 3 (and possibly 7) makes ML-IAP a potent inhibitor for a large variety of death inducing agents and events.

The occurrence of ML-IAP-specific antibodies before enrollment in the trial may have been triggered at an early stage of the melanoma or during breast cancer, however, no plasma samples prior to August 1996 were available to us. Plasma samples from 60 healthy blood donors (26 female, 34 male) failed to yield a signal above background levels. This result demonstrates the occurrence of high-titre antibodies against ML-IAP is not common in healthy individuals and supports the hypothesis of an malignancy-elicited event.

The overall IgG levels against ML-IAP increased each time after the patient received the vaccine except for late in 2000, when the patient's health deterioated rapidly until her death in March 2001 (Fig. 8 A). A serial dilution ELISA revealed that the highest titre measured, in September 1999, represents a four-fold increase over the pre-treatment sample from August 1996.

We then examined the chronological changes in the ML-IAP-specific isotypes. The level of ML-IAP-specific IgG1 antibody followed the curve for overall IgG closely (Fig. 8 B). As seen in the overall IgG curve, the titre increased each time the patient received vaccine, except for the last round of vaccination. Despite using IgG2- and IgG3-specific secondary mAbs from two different manufacturers we were unable to detect any ML-IAP-specific antibodies of these two isotypes in any of the samples. Since the mAbs used for the detection of isotypes proved to be much less sensitive than the polyclonal antibody used for detecting overall IgG concentration, it cannot be completely ruled out that anti-ML-IAP IgG2 and IgG3 antibodies were present in the patient's blood.

When we analysed the patient's serum for ML-IAP-specific IgG4 antibodies we were able to observe isotype switching after the patient started to receive vaccine (Fig. 8 C). The chronological mapping of the IgG4 concentration is distinctively different from the curve for IgG1. While there was no or very little anti-ML-IAP IgG4 present upon enrollment in the autumn of 1996, in summer of 1997 a significant and rising concentration was detected after the patient received a second round of vaccination.

As an internal control we used a commercially available allergenic extract from candida. Individuals usually have measurable antibody concentrations in their serum against this type of yeast. The patient's antibody titre against candida did not bear resemblance to the anti-ML-IAP curve ruling out that changes in antibody levels against ML-IAP could be attributed to different processing of the plasma samples (data not shown).

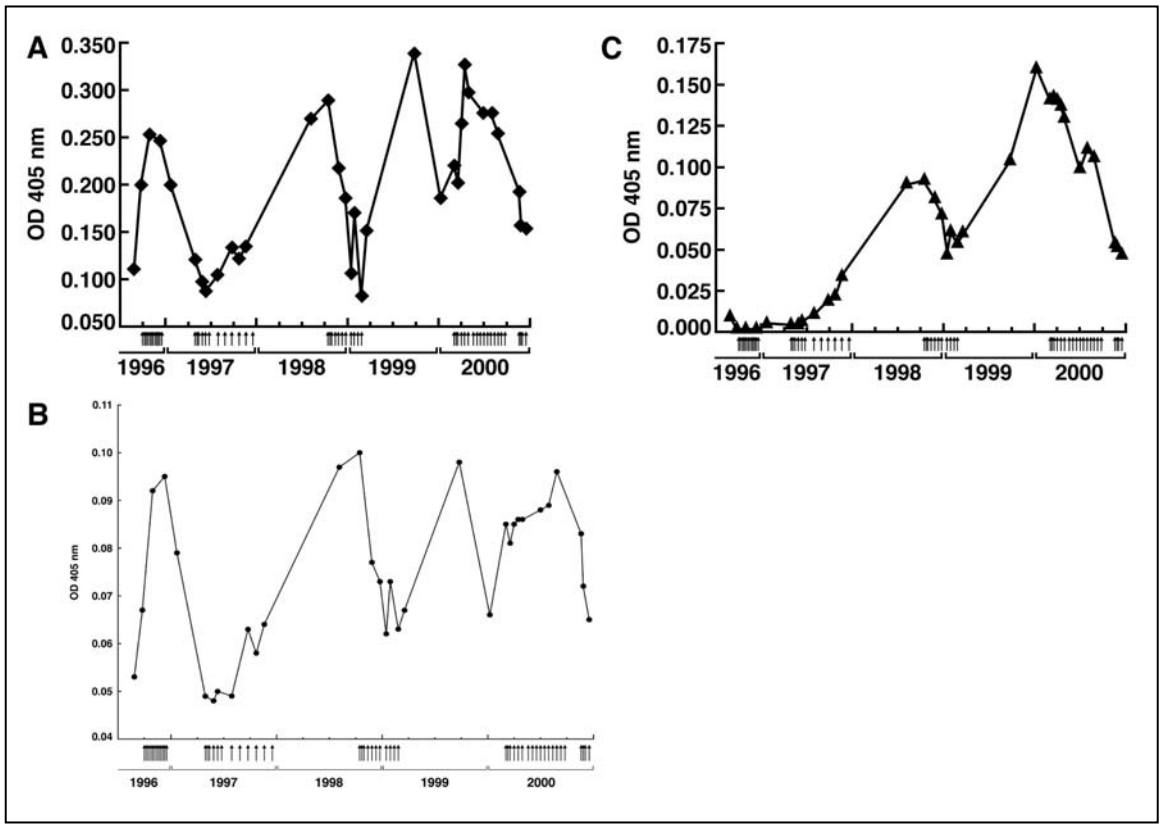

Figure 8. Vaccination augmented anti-ML-IAP antibody titers and induced isotype switching. **(A)** pan-IgG. **(B)** IgG1. **(C)** IgG4. The ELISA was performed with recombinant GST-ML-IAP protein and K030 sera diluted 1:10,000 for the pan-IgG determinations and 1:100 for the IgG1 and IgG4 measurements. A HRP-labelled polyclonal goat anti-human antibody was used for detection of pan-IgG, HRP-labelled mouse anti-human mAbs were used for detection of IgG1 and IgG4. Small arrows denote vaccinations. No reactivity against recombinant GST alone was detected.

3.4 Vaccine-Induced CD4$^+$ TILs Show Strong Proliferative Response in the Presence of Recombinant ML-IAP

Since the secretion of IgG antibodies and isotype switching is T cell dependent and since we observed brisk T lymphocyte infiltrates in the patient's tumour tissue in response to the vaccination, we were interested in studying whether ML-IAP specific CD4$^+$ T cells were present. (The following work was done in close collaboration with Robert H. Vonderheide, Joachim L. Schultze, Kara Hoar and Britta Maecker. The T cell assays in this section were carried out by their

laboratory with the author involved in planning and evaluating the experiments and providing reagents such as cell lines and purified recombinant protein.)

In order to obtain a predominantly T helper cell population $CD8^-$ T cells were separated with fluorescence activated cell sorting (FACS) from the infiltrate in the patient's calf metastasis. The sorted cells were expanded for four weeks in the presence of IL-2. Subsequent flow cytometry analysis showed that after four weeks the population was 95% $CD4^+$ T cells. We found that these cells were strongly proliferating in the presence of recombinant GST-ML-IAP protein when we carried out a tritium-labelled thymidine incorporation assay, while this was not the case with GST alone (Fig. 9 A). Also, $CD4^+$ T cells from a healthy donor failed to proliferate in the presence of the ML-IAP fusion protein, but they strongly reacted to CD3-crosslinking. Therefore the proliferative response was not triggered by bacterial contaminants present in the GST-ML-IAP protein batch.

Taken together our results strongly suggest the presence of ML-IAP specific $CD4^+$ T cells among the TILs. Additional studies regarding the cytokine profile should be carried out in order to extend this finding.

3.5 Vaccine Induced $CD8^+$ TIL Are ML-IAP-Specific And Kill ML-IAP Positive Target Cells

Activated $CD8^+$ T cells can effectively kill tumour cells. Because we observed intensive $CD8^+$ staining lymphocytes among the tumour infiltrating cells in paraffin embedded tissue sections, we were interested in determining whether they are ML-IAP specific. (For the following work we collaborated with Robert H. Vonderheide, Joachim L. Schultze, Kara Hoar and Britta Maecker. The experimental work in this section involving T cell assays was carried out by their laboratory with the author involved in planning and evaluating the experiments. The author performed the IFN-γ stimulation, the MHC class II flow cytometry analysis and provided reagents such as the transfected target cell line.)

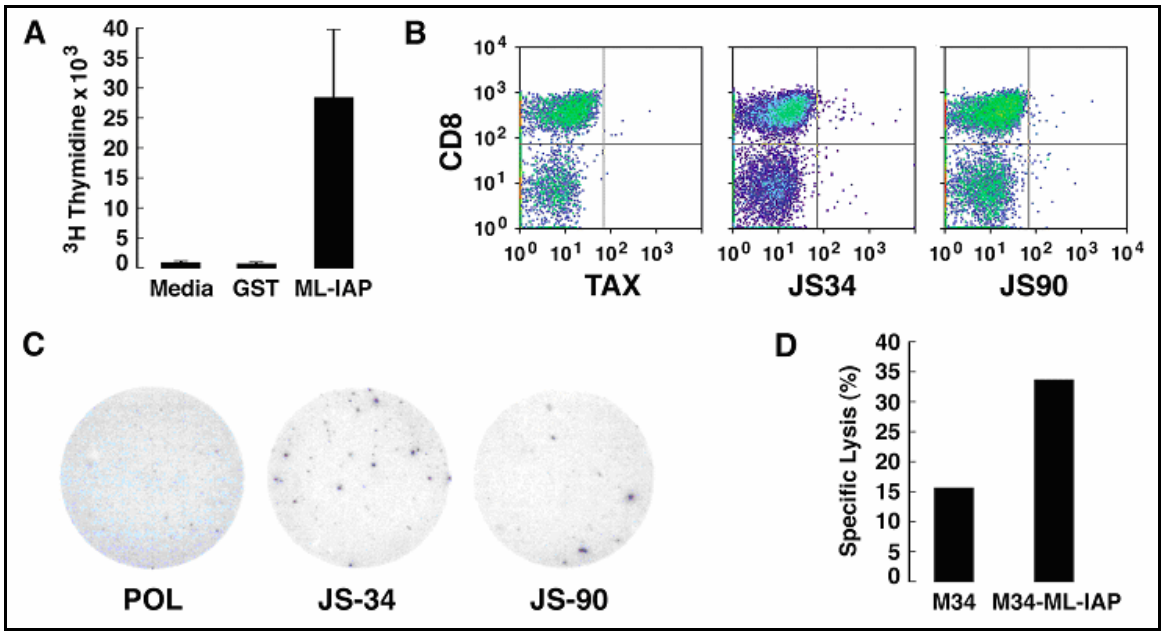

Figure 9. **(A)** Proliferative response from CD4$^+$ T cells derived from the calf metastasis in the presence of recombinant ML-IAP protein or media alone. **(B)** Tetramer staining of CD8$^+$ T cells derived from the colon metastasis. Percentage of tetramer stained CD8$^+$ T cells was 0.38 with Tax (negative control), 1.01 with JS-34 and 0.86 with JS-90. **(C)** ELISPOT assay. ML-IAP peptides JS-34 and JS-90 elicited IFN-γ secretion from CD8$^+$ T cells derived from the colon metastasis. Number of spots with Pol peptide (negative control) 0, 3; with JS-34 20, 4, 10; with JS-90 3, 7, 6. **(D)** T cells derived from the calf metastasis showed ML-IAP specific-killing (effector to target ratio of 30:1) in a cytotoxicity assay.

We analysed the ML-IAP amino acid sequence with computer algorithms that predict peptide binding to HLA-A201 [205]. Two of the determined peptides, JS-34 (SLGSPVLGL) and JS-90 (RLASFYDWPL), showed binding in a T2 cell assay.

The two tetramers with ML-IAP-derived peptides along with a tetramer with a HTLV-1 tax-derived peptide as a negative control were used to stain single cell suspensions from the patient's infiltrated metastases. It is important to note that these cells had not been expanded *in vitro*. Among the CD8$^+$/CD3$^+$ positive cells from the colon metastasis was a population that could be stained with the JS-34 tetramer, JS-90 gave a weaker staining (Fig. 9 B). Only minimal staining was seen with the HTLV-1 tax tetramer. As another control MAGE-3- and telomerase-

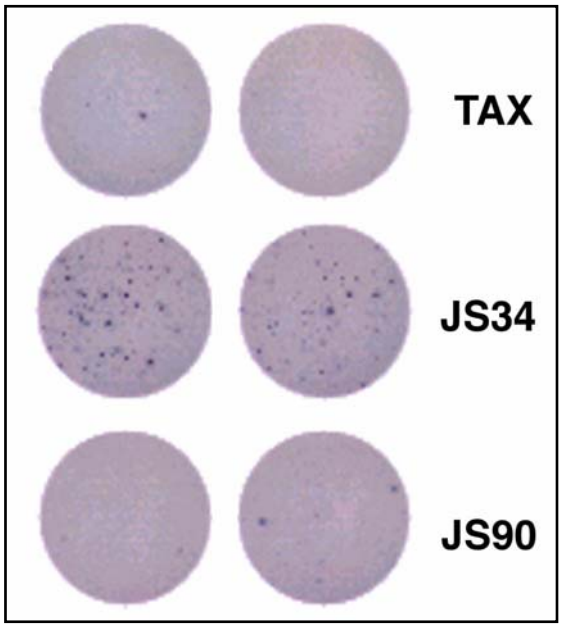

Figure 10. ELISPOT assay. ML-IAP peptide JS-34 elicited IFN-γ secretion from $CD8^+$ T cells in the calf metastasis. Number of spots with Tax peptide (negative control) 2, 0; number of spots with JS-34 36, 20; number of spots with JS-90 1, 2.

specific T cell lines derived from three HLA-A2 positive healthy donors' PBMCs were analysed with the ML-IAP tetramers. No staining was observed (data not shown). The JS-34 and the JS-90 tetramers also stained a $CD8^-$, $CD3^+$ population (seen in the lower right quadrant of Fig. 9 B) whose relevance is currently not known.

In order to verify these results with another experimental approach we tested peptide induced T cell activation by carrying out an ELISPOT assay. As in the tetramer staining we used calf metastasis-derived single cell suspensions. These cells were used without *in vitro* stimulation. Confirming our previous data, we found that incubation with peptide JS-34 and to a lesser extent with peptide JS-90 resulted in IFN-γ secretion (Fig. 9 C). IFN-γ secretion was also elicited when peptide JS-34 was incubated with colon metastases dervived cells (Fig. 10).

Finally, we wanted to examine whether $CD8^+$ TILs can lyse ML-IAP expressing targets in a specific fashion. Since the autologous calf metastasis derived melanoma cell line M34 did only express very low levels of ML-IAP (Fig. 11 and Fig. 14) we constructed an autologous ML-IAP expressing melanoma cell line. We cloned the full length 280 aa ML-IAP ORF into the retroviral vector pMFG and produced high titre VSV-G pseudotyped viral particles with the packaging cell line 293 GPG [166]. Expression of ML-IAP after infection was evaluated with an immunoblot (Fig. 10). We cultured the metastasis derived single cell suspension in the presence of IL-2 and irradiated M34 ML-IAP for three weeks in order to expand the number of ML-IAP-specific CTLs. The cytotoxicity assay showed some killing of the original autologous melanoma cell line M34, which is likely due to the recognition of the low-level expressed ML-IAP and probably also of other antigens by the TILs. There is significantly increased lysis of the ML-IAP-transduced M34 cell line (Fig. 9 D).

The killing of the ML-IAP positive targets was highly likely to be due to MHC class I T cell receptor interaction since no MHC class II expression was detected with flow cytometry on resting M34 cells or IFN-γ-treated M34 cells (data not shown). Experiments with an MHC class I blocking antibody could not be performed because of the very limited number of cells.

3.6 Emergence of ML-IAP Loss Tumour Cell Variants Correlates with Lack of TILs, Absence of Tumour Necrosis and Overall Clinical Deterioration

Since we were interested in examining ML-IAP expression patterns in normal and malignant tissue, we produced an ML-IAP-specific mAb that can be used for immunohistochemistry. Initially, we wanted to learn more about ML-IAP expression in patient K030's lesions and whether the expression level was altered during treatment.

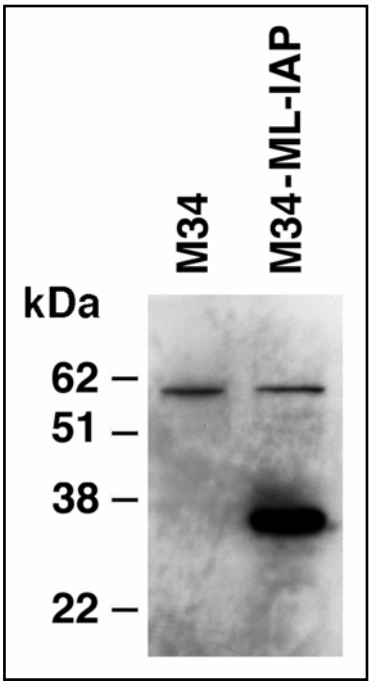

Figure 11. The monoclonal antibody 3F9 specifically recognises ML-IAP. Whole cell lysates from M34 wild type and M34 transduced with p-MFG-ML-IAP (280 aa form) retroviral supernatants were analysed in an immunoblot with mAb 3F9. (The molecular weight of the 280 aa ML-IAP splice variant is 30.8 kDa.)

We stained paraffin-embedded tissue samples from the patient's metastases with our mAb 3F9 (Fig. 12). (The staining was carried out by the technical staff of the Brigham and Women's Dept. of Pathology under the supervision of Jeffrey L. Kutok.) We observed a loss of ML-IAP expression on the melanoma cells during the course of treatment. A colon metastasis from February 1997 showed ubiquitous staining and a calf metastasis that had been resected in September 1998 showed even stronger staining of almost all cells. In December 1999 a resected subcutaneous/lymph tissue lesion, however, showed the emergence of a ML-IAP-negative tumour cell population. Finally, in September 2000 the melanoma cells from a small bowel metastasis showed no ML-IAP expression. Interestingly, this resected tissue specimen did not show any signs of lymphocyte infiltration and no necrosis was observed. Moreover, at this time the patient's health deteriorated rapidly leading to death in March 2001.

We wanted to examine whether other IAP family members compensated for the loss of ML-IAP expression. Staining of the tissue with mAbs specific for survivin and XIAP was carried out, however, no elevated expression levels were found (data not shown).

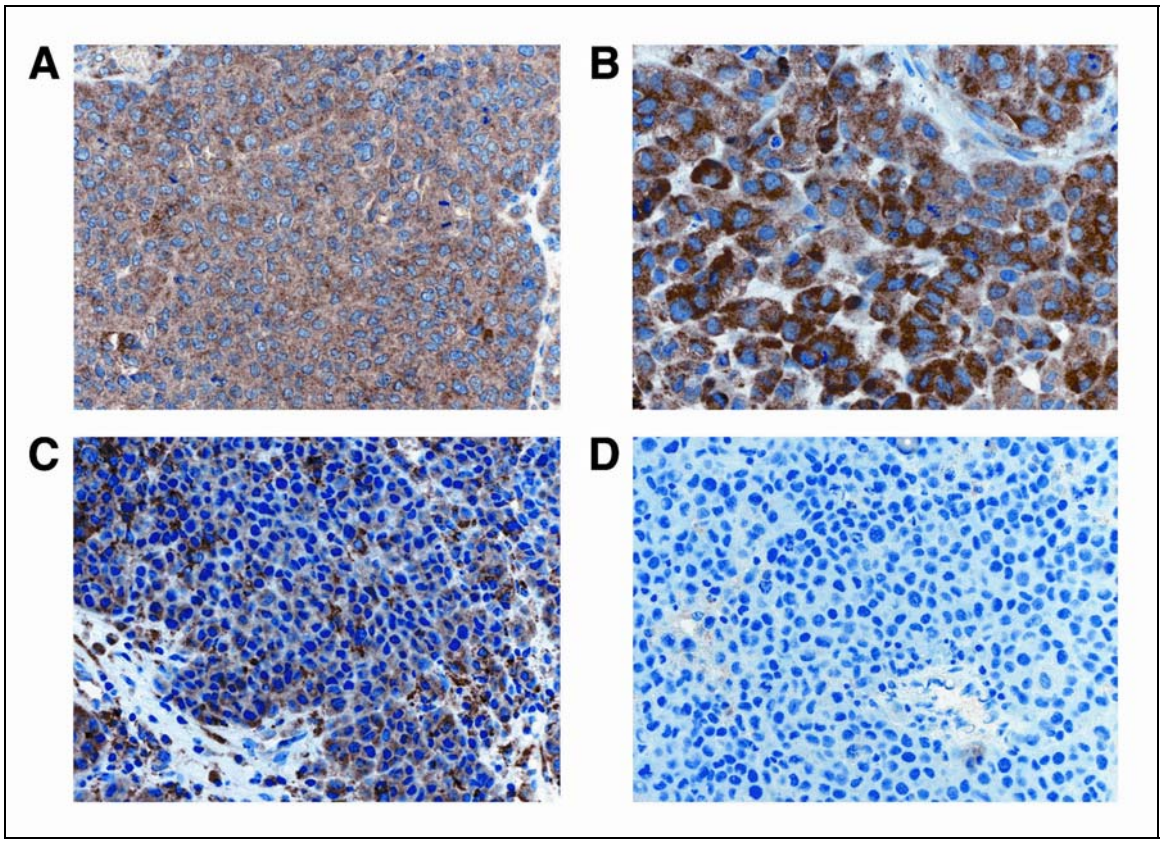

Figure 12. Vaccination stimulated the emergence of ML-IAP negative tumour cells. **(A)** Colon metastasis, resected 02/1997. **(B)** Calf metastasis, resected 09/1998. **(C)** Subcutaneous/lymph node metastasis, resected 12/1999. **(D)** Small bowel metastasis, resected 09/2000. The sections were stained with the 3F9 anti-ML-IAP monoclonal antibody and then counterstained with hematoxylin.

3.7 ML-IAP Is Widely Expressed In Neoplasms

Other studies as well as our own research documented high ML-IAP expression levels in the majority melanoma cell lines (Fig. 13) while normal melanocytes tested negative by RT-PCR [173]. We used our anti-ML-IAP mAb 3F9 to investigate the expression of ML-IAP in malignancies other than melanoma by carrying out immunohistochemistry on paraffin-embedded tissue and commercially available tissue arrays.

Preliminary data confirmed our earlier findings with the multiple tissue Northern blot. ML-IAP expression is restricted in normal tissue and was observed in testis, spinal cord, tonsils and placenta (Fig. 14 A and B and data not shown). Scoring of the cancer tissue array showed that ML-IAP is expressed in many malignancies such as lung, prostate, breast, ovarian and colon cancer. Interestingly, the chromosomal location of ML-IAP, 20q13, has been found to be frequently amplified in several types of neoplasms, among them breast, ovarian, cervical and colorectal cancer [206-211]. We also tested several samples of B cell lymphoma which tested strongly positive (Fig. 14 C and D), while a tonsil sample only showed staining of singular cells with plasmacytoid features (Fig. 14 A and B, courtesy of Jeffrey L. Kutok.) Previous findings demonstrated the presence of ML-IAP transcripts in a lymphoblastic leukaemia line and a Burkitt's lymphoma line [173].

When we performed an immunoblot on several established cancer cell lines we were able to detect the presence of ML-IAP in two B cell lymphoma lines, a leukaemia line, a cervical adenocarcinoma line and a lung carcinoma line (Fig. 15). A comparison with ML-IAP-positive melanoma line G361 reveals that the expression levels are significantly lower than in most melanoma lines.

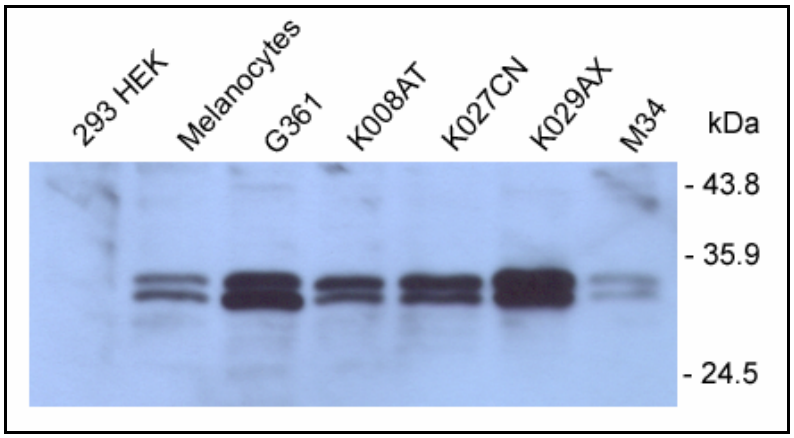

Figure 13. Expression of ML-IAP in different melanoma cell lines. 50 µg lysate per lane were run on a 10% SDS gel, blotted and then incubated with the commercially available antibody 88C570. A secondary HRP-labelled polyclonal goat anti-mouse antibody was used for detection. Lysates from melanoma lines G361 (from ATCC), K008AT, K027CN and K029AX (three lines from three patients' melanoma metastases) tested positive with an anti-ML-IAP mAb. Patient K030's cell line M34 is weakly positive. The molecular weight of the double band seen corresponds with the molecular weight of 32.8 kDa and 30.8 kDa of the two ML-IAP isoforms. The transformed human embryonic kidney cell line 293 HEK is shown as a negative control. Cultured melanocytes, which tested positive, differ from their counterparts *in situ* in both morphology and proliferative behaviour.

3.8 Cancer Patients Have Elevated Anti-ML-IAP Antibody Levels

After extensively studying patient K030 and after observing that ML-IAP is widely expressed in solid and haematologic malignancies we were interested whether other cancer patients revealed humoral activity directed against ML-IAP. For this purpose we tested post-vaccination serum samples from the remaining 32 patients enrolled in the melanoma retroviral trial and from 19 melanoma patients in our adenoviral phase I study. Additionally we tested 15 lung cancer patients enrolled in our clinical adenoviral vaccine study (Fig. 16) and used sera from healthy donors as a control. No patient in the first group beside K030 had significant levels of anti-ML-IAP IgG antibody. Interestingly, all three established

melanoma cell lines tested from patients in the retroviral trial, K008AT, K027CN and K029AX, tested positive with an anti-ML-IAP mAb in immunoblotting (Fig. 13). A fourth, metastasis-derived cell line from patient K030 (M34) tested weakly positive.

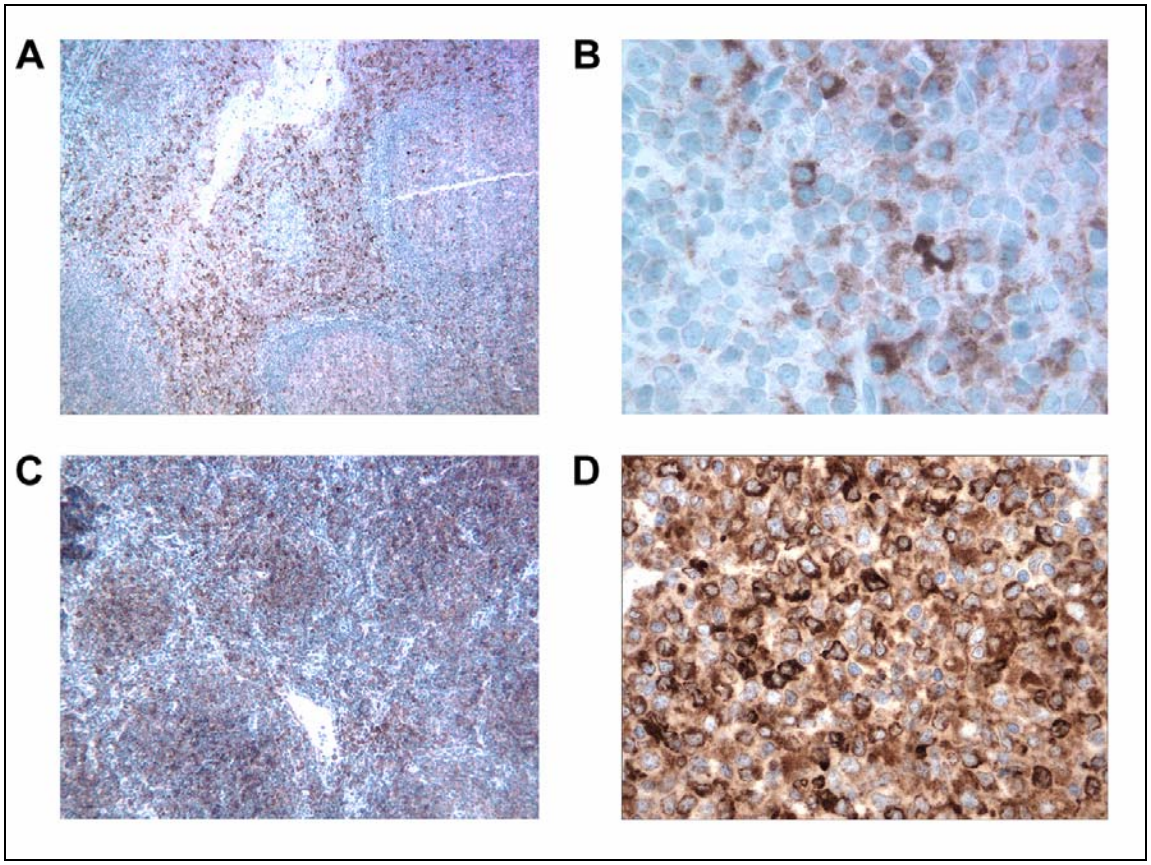

Figure 14. ML-IAP expression in tonsil and lymphoma tissue. Praffin-embedded tissue sections were tested for ML-IAP expression with our mAb 3F9 and then counterstained with hematoxilin. (A) Low power magnification of tonsil tissue. Only few individual cells are stained in the germinal centres, some cells in the mantle zone are ML-IAP-positive. (B) High power magnification of tonsil tissue. ML-IAP-positive cells have plasmacytoid features. (C) Low power magnification of a follicular lymphoma. Strong staining is visible, especially in the malignant centres. (D) High power magnification of a B cell lymphoma shows ML-IAP-positive cells have plasmacytoid features.

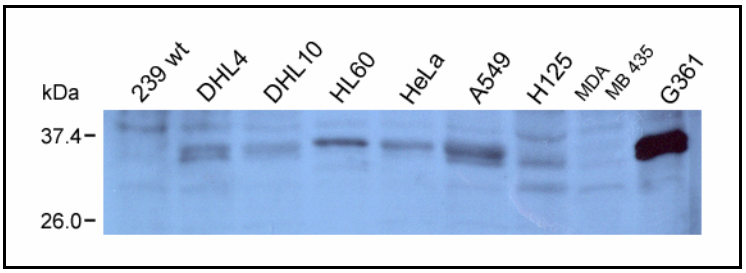

Figure 15. An immunoblot reveals ML-IAP expression in several tumour cell lines of different origin. 75 µg protein lysate were run on a 10% polyacrylamide SDS gel, blotted and probed with an anti-ML-IAP mAb (88C570). A secondary HRP-labelled polyclonal goat anti-mouse Ab was used for detection. DHL4 and DHL10 are derived from B cell lymphomas, HL60 from an acute promyelocytic leukemia, HeLa from cervical adenocarcinoma, A549 and H125 from lung cancer and MDA MB 435 from breast cancer. The transformed human embryonic kidney line 293 and melanoma line G361 were run as negative and positive controls, respectively. The longer form of ML-IAP is 32.8 kDa, the shorter form is 30.8 kDa.

When we surveyed plasma samples from patients on the adenoviral melanoma and lung cancer trials, two more patients with IgG antibodies specific for ML-IAP were identified. One melanoma patient (M21) and one lung cancer patient (L1) had significant but lower IgG titres than patient K030 as seen with the pan-IgG secondary antibody. Both patients had significant anti-ML-IAP reactivity prior to enrolling in the vaccine trials. Unfortunately, only few plasma samples were available to us from the two patients so that a chronological mapping of the ML-IAP specific humoral response during treatment was not possible. M21 had significant titres of IgG1 and, interestingly, also had significant titres of IgG4 (data not shown). Studying the antibodies' isotype in lung cancer patient L1 was not possible since the assay system did not detect measurable levels above background.

Moreover, we tested 25 serum samples of late stage prostate cancer patients. Two of the specimen had slightly elevated anti-ML-IAP antibody levels when compared to healthy blood donors (Fig. 17). Interestingly, overall the cancer patients showed slightly elevated antibody levels. While 50 healthy

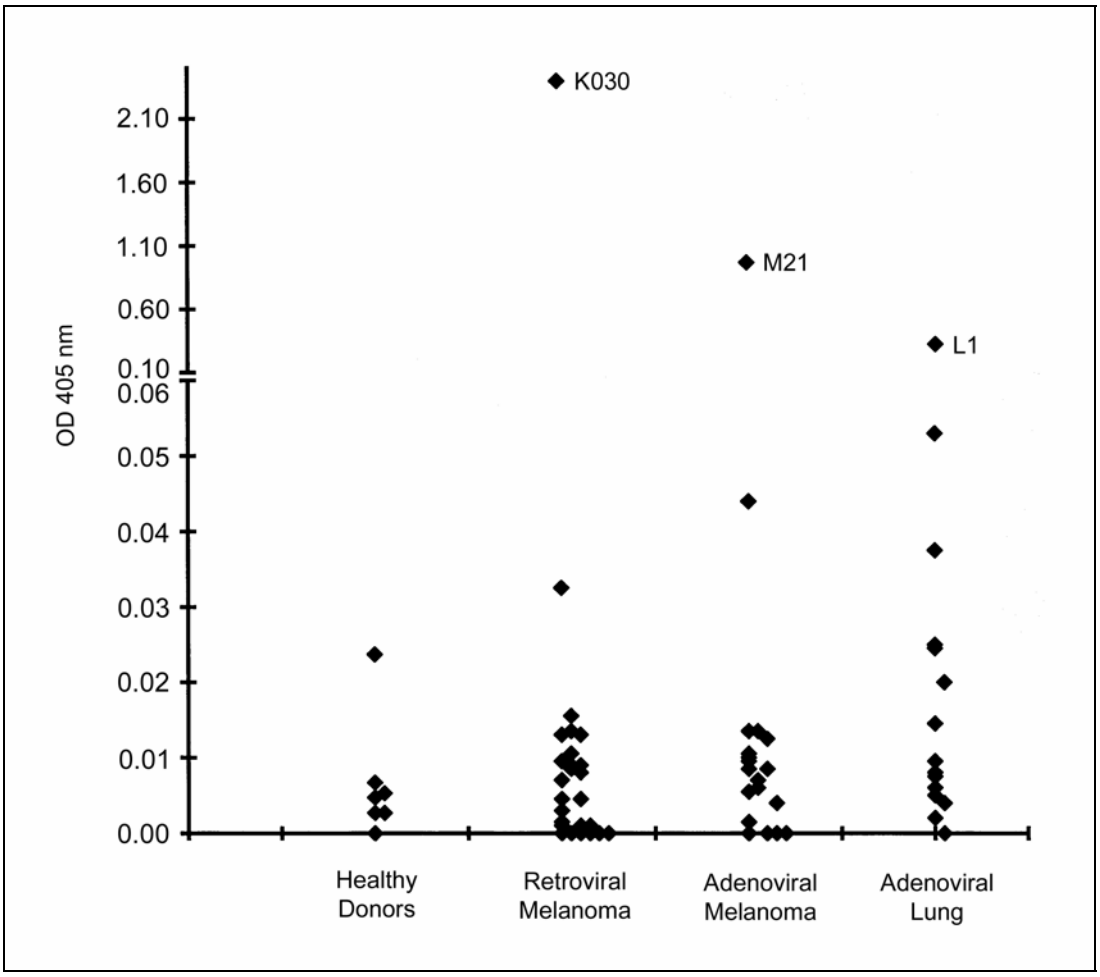

Figure 16. Anti-ML-IAP antibody levels in the plasma of healthy blood donors and melanoma and lung cancer patients enrolled in the GVAX retroviral and adenoviral phase I studies. All plasma specimen from cancer patients were obtained post-vaccination. Plasma was diluted 1:200 and incubated with recombinant GST and GST-ML-IAP-coated ELISA plates. A secondary AP-labelled polyclonal goat anti-human pan-IgG was used for detection. OD values for GST only were deducted from OD values of GST-ML-IAP.

Most healthy donors and most cancer patients showed very values within the background range. Patient K030 had by far the highest antibody level; one more melanoma patient (M21) and one lung cancer patient (L1) were found to have high anti-ML-IAP activity. There is a tendency among cancer patients to have slightly elevated antibody levels when compared to healthy donors. The y-axis has been split to allow better presentation of the data points. Above an OD (405 nm) of 1.0 the correlation between antibody concentration and absorption is not linear.

donors had a mean OD at 405 nm of 0.002, the 25 cancer patients had a mean of 0.017 Studies with breast cancer patients are currently ongoing.

While none of the 67 healthy blood donors tested so far showed significant anti-ML-IAP reactivity in our ELISA system, each of the four patient groups studied (a total of 92 cancer patients) had indicators of increased anti-ML-IAP antibodies. Our findings in lung and prostate cancer patients suggest that ML-IAP is immunogenic in other neoplasms.

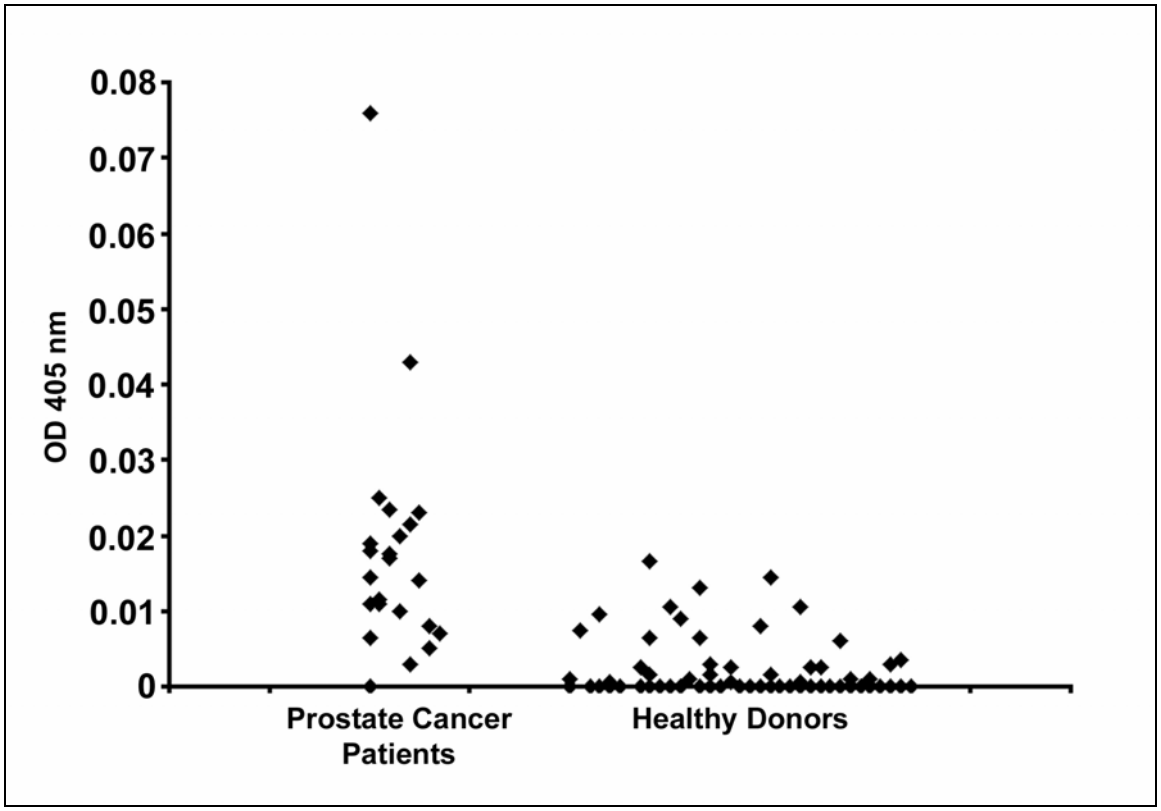

Figure 17. Anti-ML-IAP antibody levels in the plasma of healthy blood donors and late stage prostate cancer patients. Plasma was diluted 1:100 and incubated with recombinant GST-ML-IAP-coated ELISA plates. A secondary AP-labelled polyclonal goat anti-human pan-IgG was used for detection. The mean OD for is 0.002 for the healthy donor group is and 0.017 for the prostate cancer patients.

3.9 Identification of a Novel RING-less ML-IAP Splice Variant

When we investigated the occurrence of ML-IAP in haematologic malignancies we identified a novel splice variant of ML-IAP in bone marrow samples of acute myeloid leukaemia (AML) patients by RT-PCR. This ML-IAP isoform, named ML-IAPint5, that we also found in melanoma cell lines contains intron 5-derived sequence that serves as a cryptic exon (Fig. 18 and Fig. 19). Since the new stop codon is within the intronic sequence, the splice variant is only 241 amino acids in length and lacks the RING domain of the two currently described isoforms of 280 and 298 amino acids.

Current results indicate that IAP family members which possess RING domains serve as E3 ligases and can ubiquitinate caspases or undergo autoubiquitination [187]. Subsequently ubiquinated proteins are targeted for proteosomal degradation. Hence RING bearing IAPs can regulate their own as well as caspase expression levels. The lack of this zinc coordinating motif may significantly influence the biologic activity of ML-IAPint5. We are currently investigating the expression profile of this isoform and the potential role in neoplasms.

3.10 Identification of Murine ML-IAP

A murine model to study the biologic role of ML-IAP and its potential role as a vaccinating agent would be of great importance. Therefore we used the proprietary Celera database of the murine genome to identify the ML-IAP homologue [212]. A search using the human exons yielded a genomic sequence with an intron/exon structure highly homologous to human ML-IAP.

```
1/1                                                 31/11
ATG GGA CCT AAA GAC AGT GCC AAG TGC CTG CAC CGT GGA CCA CAG CCG AGC CAC TGG GCA
M   G   P   K   D   S   A   K   C   L   H   R   G   P   Q   P   S   H   W   A
61/21                                               91/31
GCC GGT GAT GGT CCC ACG CAG GAG CGC TGT GGA CCC CGC TCT CTG GGC AGC CCT GTC CTA
A   G   D   G   P   T   Q   E   R   C   G   P   R   S   L   G   S   P   V   L
121/41                                              151/51
GGC CTG GAC ACC TGC AGA GCC TGG GAC CAC GTG GAT GGG CAG ATC CTG GGC CAG CTG CGG
G   L   D   T   C   R   A   W   D   H   V   D   G   Q   I   L   G   Q   L   R
181/61                                              211/71
CCC CTG ACA GAG GAG GAA GAG GAG GAG GGC GCC GGG GCC ACC TTG TCC AGG GGG CCT GCC
P   L   T   E   E   E   E   E   E   G   A   G   A   T   L   S   R   G   P   A
241/81                                              271/91
TTC CCC GGC ATG GGC TCT GAG GAG TTG CGT CTG GCC TCC TTC TAT GAC TGG CCG CTG ACT
F   P   G   M   G   S   E   E   L   R   L   A   S   F   Y   D   W   P   L   T
301/101                                             331/111
GCT GAG GTG CCA CCC GAG CTG CTG GCT GCT GCC GGC TTC TTC CAC ACA GGC CAT CAG GAC
A   E   V   P   P   E   L   L   A   A   A   G   F   F   H   T   G   H   Q   D
361/121                                             391/131
AAG GTG AGG TGC TTC TTC TGC TAT GGG GGC CTG CAG AGC TGG AAG CGC GGG GAC GAC CCC
K   V   R   C   F   F   C   Y   G   G   L   Q   S   W   K   R   G   D   D   P
421/141                                             451/151
TGG ACG GAG CAT GCC AAG TGG TTC CCC AGC TGT CAG TTC CTG CTC CGG TCA AAA GGA AGA
W   T   E   H   A   K   W   F   P   S   C   Q   F   L   L   R   S   K   G   R
481/161                                             511/171
GAC TTT GTC CAC AGT GTG CAG GAG ACT CAC TCC CAG CTG CTG GGC TCC TGG GAC CCG TGG
D   F   V   H   S   V   Q   E   T   H   S   Q   L   L   G   S   W   D   P   W
541/181                                             571/191
GAA GAA CCG GAA GAC GCA GCC CCT GTG GCC CCC TCC GTC CCT GCC TCT GGG TAC CCT GAG
E   E   P   E   D   A   A   P   V   A   P   S   V   P   A   S   G   Y   P   E
601/201                                             631/211
CTG CCC ACA CCC AGG AGA GAG GTC CAG TCT GAA AGT GCC CAG GAG CCA GGT GCA GGC CCG
L   P   T   P   R   R   E   V   Q   S   E   S   A   Q   E   P   G   A   G   P
661/221                                             691/231
GGA CCC CCT GGG GTG AGG GCT GGG GCA GGG GAG GGC TGG GGG ACC CCG ACC TTC CAT GGC
G   P   P   G   V   R   A   G   A   G   E   G   W   G   T   P   T   F   H   G
721/241
CCA TAG
P   *
```

Figure 18. Sequence of ML-IAPint5 which retains part of intron 5 as a cryptic exon. The BIR domain is marked by red letters, the intron 5 derived sequence is underlined. The RING domain is missing in this splice variant.

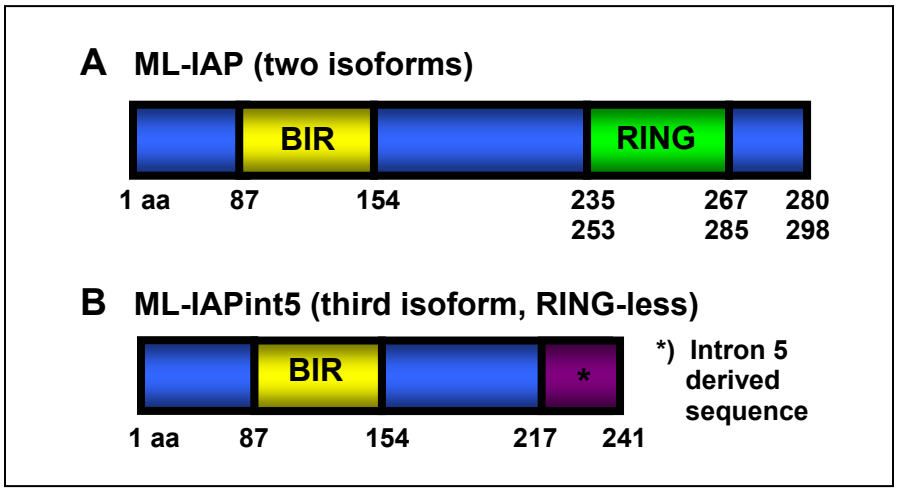

Figure 19. Schematic comparison of the two currently described ML-IAP isoforms **(A)** with the shorter splice variant that retains intronic sequence as a cryptic exon **(B)**. The shorter (241 amino acids) form of ML-IAP lacks a RING domain that functions as an E3 ligase in ubiquitination.

In order to verify the database-derived sequence we carried out a series of nested RT-PCRs with cDNA derived from the murine melanoma cell line B16. An amplified band was excised, cloned and sequenced (Fig. 20). The PCR derived sequence was identical to the sequence found by homology search in the murine genome.

A comparison of the 280 aa human ML-IAP and the 271 aa murine ML-IAP reveals overall 68% identity (74% positives) with the highest degree of homology in the BIR and RING regions (Fig. 21). All consenus motifs within these two zinc coordinating domains are conserved. Functional studies and analysis of the tissue distribution are pending.

```
1/1                                                 31/11
ATG GGG CCT GAG AGT AGG GCC AGG GAC TCG GTC CGT GGC CCA GAA CTA AGC CAC AGG GAA
M   G   P   E   S   R   A   R   D   S   V   R   G   P   E   L   S   H   R   E
61/21                                               91/31
GAT GGC AGT GGC CGC ACA CAG GAA CAG GAT AAA CCC CAC TGT CCG TGT AAC CAT GTC CTG
D   G   S   G   R   T   Q   E   Q   D   K   P   H   C   P   C   N   H   V   L
121/41                                              151/51
GGC CAG GAC TGC CTA GAT GGG CAG ATC TTA GGC CAG CTT CGG CCT CTG TCA GAA GAG GAA
G   Q   D   C   L   D   G   Q   I   L   G   Q   L   R   P   L   S   E   E   E
181/61                                              211/71
GAA TCC TCT GGG GCT GCC TTC CTT GGG GAG CCT GCC TTC CCT GAG ATG GAC TCA GAG GAT
E   S   S   G   A   A   F   L   G   E   P   A   F   P   E   M   D   S   E   D
241/81                                              271/91
CTC CGG CTA GCC TCC TTC TAC GAC TGG CCA TCT ACT GCA GGG ATT CAG CCT GAG CCA TTG
L   R   L   A   S   F   Y   D   W   P   S   T   A   G   I   Q   P   E   P   L
301/101                                             331/111
GCT GCT GCT GGG TTC TTC CAC ACA GGC CAG CAG GAC AAG GTG AGA TGT TTC TTC TGC TAT
A   A   A   G   F   F   H   T   G   Q   Q   D   K   V   R   C   F   F   C   Y
361/121                                             391/131
GGG GGT CTA CAG AGC TGG GAG CGT GGG GAT GAC CCC TGG ACA GAG CAT GCC CGA TGG TGT
G   G   L   Q   S   W   E   R   G   D   D   P   W   T   E   H   A   R   W   C
421/141                                             451/151
CAG TTC CTG CTA CGG TCA AAA GGA AGG GAC TTT GTG GAA AGA ATC CAG ACC TAC ACC CCT
Q   F   L   L   R   S   K   G   R   D   F   V   E   R   I   Q   T   Y   T   P
481/161                                             511/171
TTG CTG GGA TCC TGG GAT CAA GGA GAA GAA CCA GAA GAT GCA GTC TCT GCC ACT CCT TCA
L   L   G   S   W   D   Q   G   E   E   P   E   D   A   V   S   A   T   P   S
541/181                                             571/191
GCT CCT GCC CAT GGA AGC CCT GAG TTA CTC AGA TCC AGA AGA GAG ACC CAG CCT GAA GAT
A   P   A   H   G   S   P   E   L   L   R   S   R   R   E   T   Q   P   E   D
601/201                                             631/211
GTC AGT GAG CCA GGA GCC AAG GAT GTT CAG GAA CAG CTG CGA CAG CTG CAG GAA GAG AGG
V   S   E   P   G   A   K   D   V   Q   E   Q   L   R   Q   L   Q   E   E   R
661/221                                             691/231
AGA TGC AAG GTG TGC CTG GAC CGA GCC GTC TCC ATA GTC TTC GTG CCC TGT GGC CAC TTC
R   C   K   V   C   L   D   R   A   V   S   I   V   F   V   P   C   G   H   F
721/241                                             751/251
GTC TGC ACC GAG TGT GCT CCC AAC CTG CAG CTG TGC CCT ATC TGC AGG GTG CCT ATC TGT
V   C   T   E   C   A   P   N   L   Q   L   C   P   I   C   R   V   P   I   C
781/261
AGC TGT GTA CGC ACA TTC CTG TCC TAA
S   C   V   R   T   F   L   S   *
```

Figure 20. Putative nucleotide and amino acid sequence of murine ML-IAP. The BIR domain is marked by red letters, the RING domain is marked by blue letters.

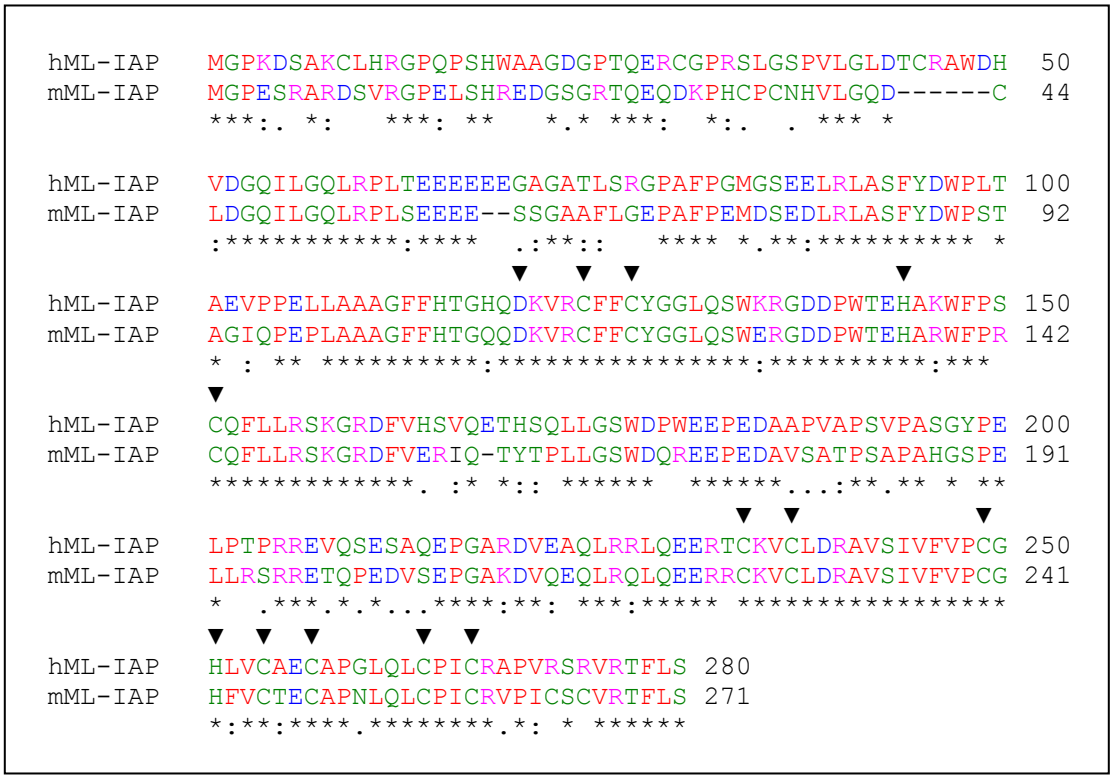

Figure 21. Comparison of the amino acid sequences of human and murine ML-IAP with Clustal W [192] reveals a high degree of similarity. 192 out of 280 residues are identical (68%), 210 out of 280 residues are positives (74%). The residues of the BIR and RING consensus motifs are marked with an "▼".

"*" denotes an identical residue, ":" denotes a conserved substitution and "." denotes a semi-conserved substitution. The colour red denotes small (small + hydrophobic (incl. aromatic - Y)) amino acids, blue denotes acidic amino acids, magneta denotes basic amino acids and green denotes hydroxyl + amine + basic – Q amino acids.